International Communications in Heat and Mass Transfer 39 (2012) 1395–1403

Contents lists available at SciVerse ScienceDirect

International Communications in Heat and Mass Transfer

journal homepage: www.elsevier.com/locate/ichmt

Analysis of turbulent flow and heat transfer over a double forward facing step with obstacles ☆

Hakan F. Oztop [a], Khudheyer S. Mushatet [b,*], İlker Yılmaz [c]

[a] Department of Mechanical Engineering, Technology Faculty, Fırat University, Elazig, Turkey
[b] Mech. Eng. Dept., Thi-qar University, Nassiriya City, Iraq
[c] Airframe and Power plant Dept., College of Aviation, Erciyes University, Kayseri, Turkey

ARTICLE INFO

Available online 21 July 2012

Keywords:
Double forward facing step
Duct flow
Turbulence
Obstacle

ABSTRACT

A numerical study has been conducted to analyze the turbulent forced convection heat transfer for double forward facing step flow with obstacles. Obstacles have rectangular cross-sectional area with different aspect ratio that is located before each step. The numerical solutions of continuity, momentum and energy equations were solved by using a commercial code which uses finite volume techniques. The effect of turbulence was modeled by using a k–ε model. The effects of step height, obstacle aspect ratio and Reynolds number on the flow and heat transfer are investigated. The obtained results show that the rate of heat transfer is enhanced as aspect ratio of obstacle increases and this trend is affected by the step height. Also the results verified that the pressure drop decreases as obstacle aspect ratio increases.

1. Introduction

Turbulent forced convection flow in channel with backward or forward facing step made the concerns of the researchers in recent years. Such flows are widely implemented in many engineering and technological application such as gas turbine, heat exchangers, combustion chambers and cooling of electronic devices. The flow over a forward facing step (FFS) has more complexities than that of backward facing step (BFS) due to the presence of more separating zones for the same flow conditions. The enhancement of heat transfer is expected to be improved in FFS. The size and strength of recirculation zones near the two steps are crucial for heat transfer enhancement. Thus, an attempt is made to insert two rectangular obstacles mounted evenly near the two steps.

A review on laminar mixed convection flow over backward and forward facing step has been performed by Abu-Mulaweh [1]. Turbulent forced convection heat transfer for double forward facing step flow is studied with a numerical method by Yılmaz and Oztop [2]. The bottom wall of the channel is heated at uniform temperature and the flow temperature at the upstream is colder than that of the wall. It is found that the second step can be used as control parameter for heat and fluid flow. Nassab et al. [3] made a calculation on turbulent flows with heat transfer over a single forward facing step. The k–ε model is employed for computation of turbulence fluctuations. They found that the coefficient of heat transfer and also the hydrodynamic behavior of the flow are strongly dependent to step length and inclination angle. A numerical investigation of entropy generation in laminar forced convection of gas flow over a recess including two inclined backward and forward facing steps in a horizontal duct under bleeding condition is presented by Bahrami and Nassab [4]. Abu-Mulaweh [5] made a study on heat transfer and fluid flow of turbulent mixed convection boundary-layer air flow over an isothermal two-dimensional, vertical forward-facing step. In his case, the upstream and downstream walls and the step itself were heated to a uniform and constant temperature. He found that the turbulence intensity of the streamwise and transverse velocity fluctuations and the intensity of temperature fluctuations downstream of the step increase as the step height increases. The separation ahead of a forward facing step was investigated by Stüer et al. [6] under laminar flow conditions using the hydrogen bubble technique to visualize and PTV to evaluate the 3D velocity field in a Eulerian representation in the vicinity of the step. An experimental investigation of the recirculation zone formed downstream of a forward facing step immersed in a turbulent boundary layer is made by Sherry et al. [7]. They discussed the mechanisms affecting the reattachment distance, namely the turbulent mixing within the boundary layer and the velocity deficit in the boundary layer. A horizontal wall jet impinging onto a forward facing step in a cross-flow is examined by Langer et al. [8]. An experimental technique is preferred by using planar laser induced fluorescence (PLIF). It is found that the entrainment coefficients, for elliptical jet case had average values of 0.15 and 0.58. Atashafrooz et al. [9] worked on entropy generation in laminar forced convection of gas flow over a recess including two inclined backward and forward facing steps in a horizontal duct under bleeding condition. Other related studies on forward facing step flow can be found in literature [10–16].

To the best knowledge of the authors, this special problem has not yet studied. The aim of the present study is to show how a rectangular

☆ Communicated by W.J. Minkowycz.

* Corresponding author.
E-mail address: khudheyer2004@yahoo.com (K.S. Mushatet).

0735-1933/$ – see front matter © 2012 Elsevier Ltd. All rights reserved.
doi:10.1016/j.icheatmasstransfer.2012.07.011

Nomenclature

Ar	obstacle aspect ratio [t/w]
G	generation term [kg m s^{-3}]
H	height of the channel [m]
k	turbulent kinetic energy [m^{-2} s^{-2}]
L	length of the channel [m]
Nu	local Nusselt number [–]
p	pressure [N m^{-2}]
Pr	Prandtl number [–]
Re	Reynolds number [–]
s	step height [m]
T_c	cold wall temperature [°C]
T_h	hot wall temperature [°C]
$\overline{\rho u_i u_j}$	Reynolds stresses [kg m s^{-2}]
$\overline{\rho u_i t_j}$	turbulent heat fluxes [kg °C m^{-2} s]
u,v	axial and normal velocity [m s^{-2}]
x,y	Cartesian coordinates [m]

Greek letters

ε	turbulence dissipation rate [m^{-2} s^{-3}]
μ	dynamic viscosity [N s m^{-2}]
μ_t	turbulent viscosity [N s m^{-2}]
ρ	air density [kg m^{-3}]

obstacle located before each step of the double forward facing step flow can affect the behavior of the flow field and consequently enhancing the rate of heat transfer.

1.1. Physical problem

The considered problem is depicted schematically in Fig. 1. It is a channel with a double forward facing (FFS). The top wall is insulated while the bottom wall and steps have a constant temperature (T_h) which is hotter than the inlet flow temperature. The heights of the double forward facing steps (FFS) are h_1 and h_2 respectively. The height and length of the channel are depicted by H and L. Here a, b and c show the lengths of bottom wall and steps while t and w represent the height and width of the obstacle. Three cases were studied as shown in Table 1. The obstacle aspect ratio was ranged from 0.5 to 1. Three values of Reynolds numbers (3×10^4, 8×10^4 and 1×10^5) were tested.

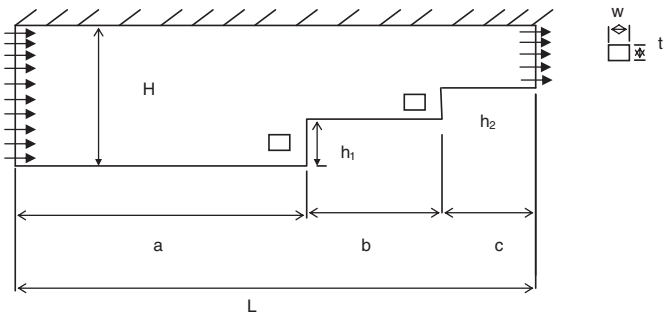

Fig. 1. Schematic diagram of physical problem, $L=1.6$ m, $a=1$ m, $b=0.2$ m, $c=0.4$ m, $H=0.1$ m.

Table 1
Studied cases.

Cases	$H_1=h_1/H$	$H_2=h_2/H$	H_1/H_2
1	0.2	0.4	0.5
2	0.4	0.6	0.65
3	0.6	0.8	0.75

2. Mathematical model and numerical analysis

The governing equations of the continuity, momentum and energy for fluid flow and heat transfer are described as follows.

$$\frac{\partial}{\partial x_i}\left(\rho U_i\right)=0 \tag{1}$$

$$\frac{\partial\left(U_iU_j\right)}{\partial x_j}=-\frac{\partial P}{\partial x_i}+\frac{\partial}{\partial x_j}\left(\mu\frac{\partial U_i}{\partial x_j}-\overline{\rho u_iu_j}\right) \tag{2}$$

$$\frac{\partial\left(U_iT_j\right)}{\partial x_j}=\frac{\partial}{\partial x_j}\left(\frac{\mu}{\Pr}\frac{\partial T_i}{\partial x_j}-\overline{\rho u_it_j}\right) \tag{3}$$

The effect of turbulence was modeled by using a k–ε model [17]. This model consists of two transport equations, one for the turbulence kinetic energy and the other for the dissipation of turbulence kinetic energy.

$$\frac{\partial\rho kU_i}{\partial x_j}=\frac{\partial}{\partial x_j}\left[\left(\mu+\frac{\mu_t}{\sigma_k}\right)\frac{\partial k}{\partial x_j}\right]+\rho(G_b-\varepsilon) \tag{4}$$

$$\frac{\partial\rho\varepsilon U_j}{\partial x_j}=\frac{\partial}{\partial x_j}\left[\left(\mu+\frac{\mu_t}{\sigma_\varepsilon}\right)\frac{\partial\varepsilon}{\partial x_j}\right]+\rho\frac{\varepsilon}{k}\left(c_{1\varepsilon}G_b-c_{2\varepsilon}\varepsilon\right) \tag{5}$$

$$G_b=\mu_t\left(\frac{\partial u_i}{\partial x_j}+\frac{\partial u_j}{\partial x_i}\right)\frac{\partial u_i}{\partial x_j} \tag{6}$$

$$\mu_t=\rho c_\mu\frac{k^2}{\varepsilon} \tag{7}$$

The values of constants in this model are σ_k, σ_ε, $C_{1\varepsilon}$, $C_{2\varepsilon}$, and C_μ as 1.0, 1.3, 1.44, 1.92, and 0.09, respectively [18].

2.1. Boundary conditions

At inlet: $u=U_{in}$, $T_{in}=293$ K
At outlet: constant pressure is imposed, $p=101{,}325$ Pa.
At the walls: no slip boundary conditions are considered. The bottom wall and steps are maintained at constant hot temperature ($T=T_h=313$ K) while the top wall is insulated.

The numerical solution of the described governing equations was done by using Fluent 6.2 software while the grid generation for the described geometry was done by using Gambit pre-Processor. The Gambit has a wide flexibility to deal with complex geometries. The simulations were tested for a range of grid densities, namely 15,761, 35,812, and 139,760 and it is found that trend of the calculated studied parameters does not change when the grid density exceeds 139,760. So this grid density has been chosen for all the simulations in the present study. The numerical convergence of the considered model was checked for every studied case depending on numerical residuals of the computed variables. The validity of the model was checked through comparison with published results (Refs. [3,16]) as shown in Figs. 13 and 14.

3. Results and discussion

A numerical study was performed for turbulent flow and heat transfer for double FFS with obstacles. The working fluid was air with Pr = 0.71. The parameters studied are the ratio of step heights (of first and second step) to channel height, aspect ratio of obstacle and Reynolds number.

Fig. 2 shows the velocity vector distribution for the studied cases with obstacle aspect ratio equal to 0.5. It can be seen that the recirculation regions are formed near the first and second steps. Inserting an obstacle near each step affected significantly the formation and shape of the resulting vortices and secondary flow. So obstacle increases the formation of eddies and that is expected to enhance the rate of heat transfer. As a general feature, the flow field initiates with uniform velocity profile and develops along the channel until impinging the obstacle near the first step. A part of the flow jumps up the obstacle and another part down the obstacle impinging it and jumps the top of the first step. A remaining flow forms a recirculation region behind the obstacle. Also a recirculation region is formed along the length of the first step; however it is less in size. The scenario is repeated near the second step. As the ratio of the step height increases, the resulting vortices and eddies increase as shown in (b) and (c).

The axial velocity profiles at different stream wise stations near the obstacle at two steps are described in Fig. 3. It is observed that the maximum value of negative velocity lies at $x = 1.15$ near the

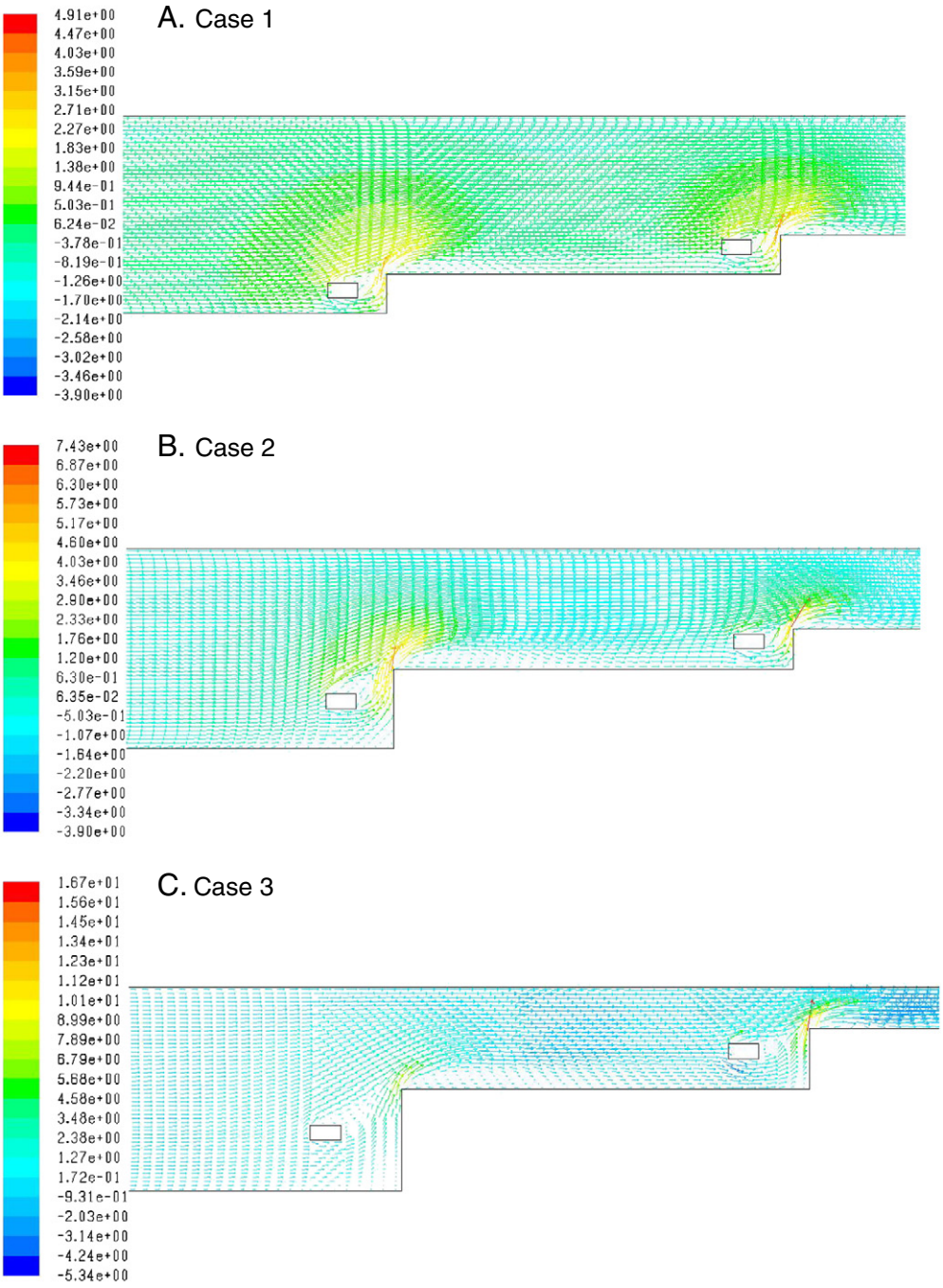

Fig. 2. Velocity vectors colored by axial velocity for different step height ratios, Ar = 0.5 and Re = 30,000.

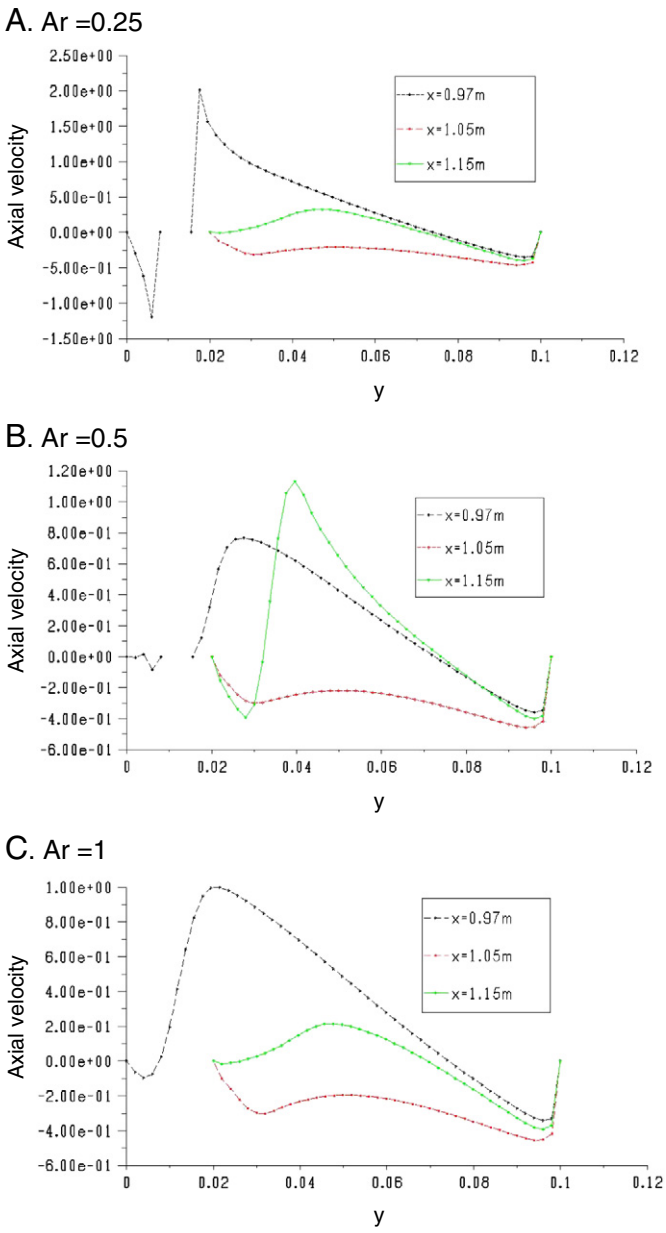

Fig. 3. Axial velocity profiles for different obstacle's aspect ratios, case 1 and Re = 30,000.

obstacle in the vicinity of the second step. This gives an indication for the recirculation which is stronger at this zone and consequently more enhancement of heat transfer is expected to be obtained.

The variation of pressure coefficient along the whole channel bottom wall for different values of obstacle aspect ratio is depicted in Fig. 4. As it is shown, the pressure coefficient is decreased as obstacle aspect ratio increases. It is observed that the pressure coefficient trend is similar at $x = 0.8$ after that it undergoes a sudden change due to the presence of circulation flow and the minimum values are recorded at the edges of the two steps ($x = 1$ and $x = 1.2$). The pressure coefficient value is less at the second step compared with the first step and that confirms the large strength of recirculation at the second step. The mentioned behavior of the pressure coefficient is dominant for all studied cases. As Reynolds number increases, the pressure coefficient is noticeably increased as shown in Fig. 5. The cause is attributed to increased size and strength of recirculation regions. This trend is found dominant for all considered obstacle aspect ratios.

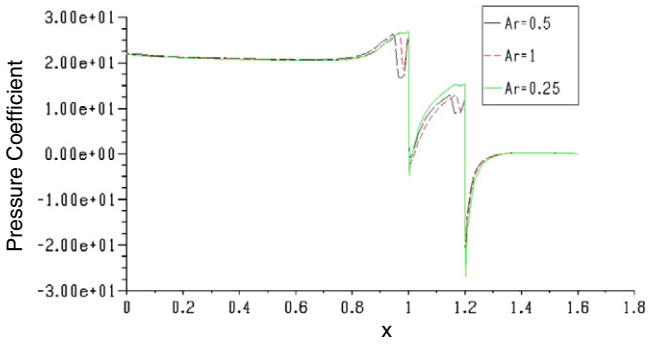

Fig. 4. Variation of pressure coefficient along the bottom wall for different obstacle's aspect ratio, case 1 and Re = 30,000.

The contours of static temperature for different obstacle aspect ratio for case 1 are depicted in Fig. 6. It is observed that the hot temp region is high near the two steps and decreased as obstacle aspect ratio increases. This is because when aspect ratio increases, the amount of mixing flow just after the obstacle is decreased and vice versa when obstacle aspect ratio increases. It is worth to mention here that the obstacle aspect ratio affects the thickness of thermal boundary layer in the vicinity of the steps. This layer seems to be thinner at the first step compared with the other step which leads to an increase in the temperature stratification and consequently increase the rate of heat transfer.

Fig. 7 shows the distribution of turbulent kinetic energy for different values of obstacle aspect ratio and case 1. It is observed that the turbulent kinetic energy is increased near the obstacles close to the two steps because of the increases of the turbulence due to flow complexity resulted by adding obstacles to the problem. Fig. 8 shows the effect of Reynolds number on distribution of path lines colored by axial velocity for case 1 and Ar = 1. It is observed that the values of negative velocities are increased and recirculation regions become larger as Reynolds number increases. This effect is larger as Reynolds number increases and this is expected to influence on enhancement of heat transfer. When Reynolds number increases, the inertia forces increase which led to an increase in the turbulence and mixing. The variation of local Nusselt number (on the whole bottom hot wall) is depicted in Figs. 9–11. It is clear that the Nusselt number trend is similar for $x \leq 0.8$ but it differs significantly near the two steps. The Nusselt number increases as aspect ratio increases and this increase is larger near the second step. This trend is dominant for the cases studied. However the maximum values of Nusselt number increase as the height of the steps increases because of the increase of blockage and hence increase

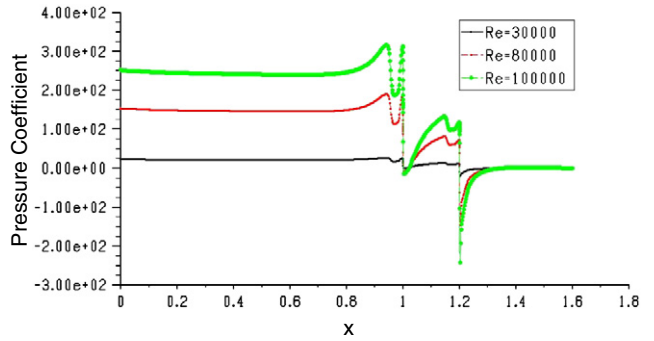

Fig. 5. Variation of pressure coefficient along the bottom wall for different values of Re, case 1 and Ar = 0.5.

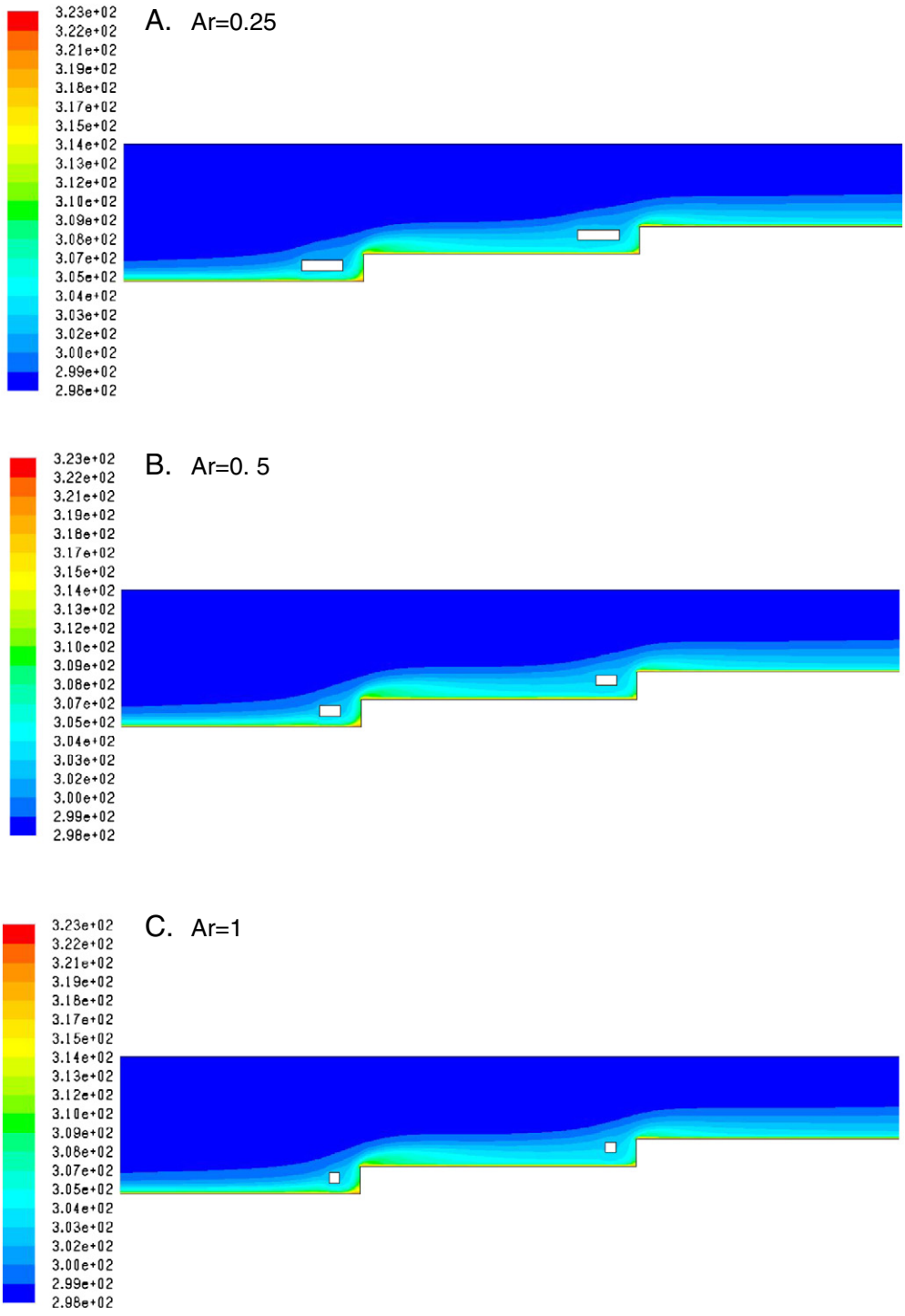

Fig. 6. Contours of static temperature for different obstacle's aspect ratios, case 1 and Re = 30,000.

of the heat losses. The effect of Reynolds number on Nusselt number variation is seen in Fig. 12. It is clear that the Nusselt number increases as Reynolds number increases due to the increase in recirculation and eddies which enhance the rate of heat transfer. This increase is enhanced as the step height increases.

The validity of the present code was tested against some published results as shown in Figs. 13 and 14. As the figures show, an acceptable agreement is obtained. However some discrepancy is observed due to the use of the k–ε model where this model gives a percentage of prediction in some of re-circulating flows.

4. Conclusions

The turbulent flow and heat transfer for a channel two forward step flow with rectangular obstacles have been numerically studied. Three cases ($A_r = 0.25$ to 1, $H_1/H_2 = 0.5$ to 0.75, Re = 30,000 to 100,000) were studied. The obtained results show that the obstacle aspect ratio is a controlling factor for enhancing the rate of heat transfer. The maximum values of Nusselt number were at Ar = 1 for the considered values of the step height. The position of these values is closer to second forward step ($x = 1.2$) rather than the first step. Also it can be

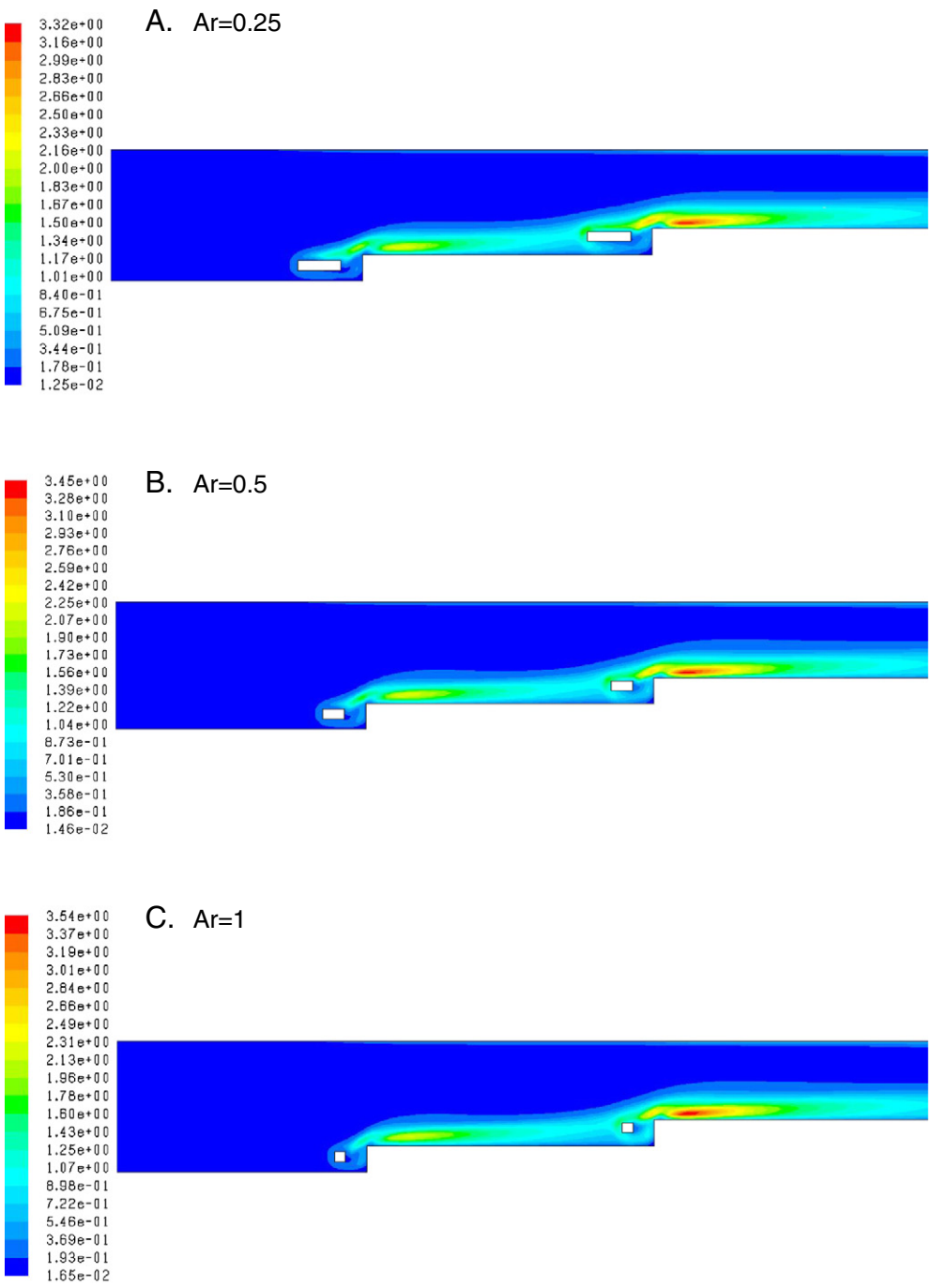

Fig. 7. Contours of turbulent kinetic energy for different obstacle's aspect ratios, case 1 and Re = 30,000.

reported that the minimum value of the pressure coefficient occurs in the vicinity of the second step for the considered parameters.

References

[1] H.I. Abu-Mulaweh, A review of research on laminar mixed convection flow over backward-and forward-facing steps, International Journal of Thermal Sciences 42 (2003) 897–909.
[2] I. Yılmaz, H.F. Oztop, Turbulence forced convection heat transfer over double forward facing step flow, International Communications in Heat and Mass Transfer 33 (2006) 508–517.
[3] S.A.G. Nassab, R. Moosavi, S.M.H. Sarvari, Turbulent forced convection flow adjacent to inclined forward step in a duct, International Journal of Thermal Sciences 48 (2009) 1319–1326.
[4] A. Bahrami, S.A.G. Nassab, Study of entropy generation in laminar forced convection flow over a forward-facing step in a duct, International Review of Mechanical Engineering 4 (2010) 399–404.
[5] H.I. Abu-Mulaweh, Turbulent mixed convection flow over a forward-facing step — the effect of step heights, International Journal of Thermal Sciences 44 (2005) 155–162.
[6] H. Stüer, A. Gyr, W. Kinzelbachv, Laminar separation on a forward facing step, European Journal of Mechanics — B/Fluids 18 (1999) 675–692.
[7] M. Sherry, D. Lo Jacono, J. Sheridan, An experimental investigation of the recirculation zone formed downstream of a forward facing step, Journal of Wind Engineering and Industrial Aerodynamics 98 (2010) 888–894.
[8] D.C. Langer, B.A. Fleck, D.J. Wilson, Trajectory measurements of a wall jet impinging onto a forward facing step entering a cross-flow, Journal of Hazardous Materials 176 (2010) 199–206.
[9] M. Atashafrooz, S.A.G. Nassab, A.B. Ansari, Numerical investigation of entropy generation in laminar forced convection flow over inclined backward and forward facing steps in a duct under bleeding condition, Thermal Science (2012), http://dx.doi.org/10.2298/TSCI110531026A.
[10] H. Hattori, Y. Nagano, Investigation of turbulent boundary layer over forward-facing step via direct numerical simulation, International Journal of Heat and Fluid Flow 31 (2010) 284–294.

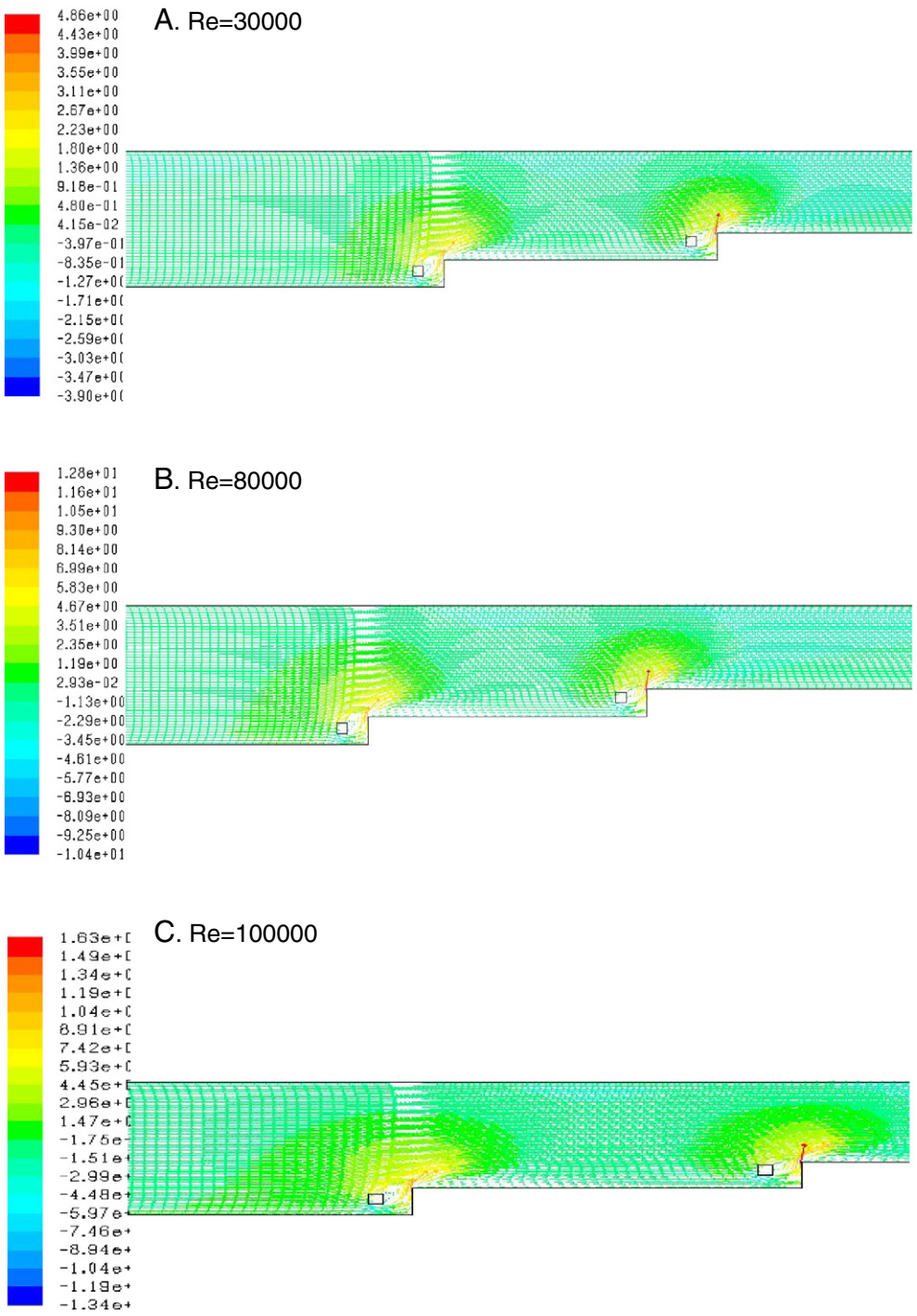

Fig. 8. Effect Re on the flow field (velocity vectors colored by axial velocity) for case 1 and Ar = 1.

[11] D. Wilhelm, C. Hartel, L. Kleiser, Computational analysis of the two-dimensional–three-dimensional transition in forward-facing step flow, Journal of Fluid Mechanics 489 (2003) 1–27.
[12] R. Camussi, M. Felli, F. Pereira, G. Aloisio, A.D. Marco, Statistical properties of wall pressure fluctuations over a forward-facing step, Physics of Fluids 20 (2008) 075113-1–075113-13.
[13] J.G. Barbosa-Saldana, N.K. Anand, Flow over a three-dimensional horizontal forward-facing step, Numerical Heat Transfer, Part A: Applications 53 (2008) 1–17.
[14] H.I. Abu-Mulaweh, B.F. Armaly, T.S. Chen, Measurements of turbulent mixed convection flow over a vertical forward-facing step, In: ASME Proceedings of the Summer Heat Transfer Conference, Las Vegas, Nevada, 2003, CD-ROM.
[15] H. Stüer, Investigation of separation on a forward facing step, PhD thesis, Swiss Federal Institute of Technology, Zürich, 1999.
[16] K. Abe, T. Kondoh, Y. Nagano, A new turbulence model for predicting fluid flow and heat transfer in separating and reattaching flows — I. Flow field calculations, International Journal of Heat and Mass Transfer 37 (1994) 139–151.
[17] Y.T. Chen, J.H. Nie, B.F. Armaly, H.T. Hsieh, Turbulent separated convection flow adjacent to backward-facing step-effects of step height, International Journal of Heat and Mass Transfer 49 (2006) 3670–3680.
[18] B.E. Launder, D.B. Spalding, The numerical computation of turbulent flows, Computer Methods in Applied Mechanics and Engineering 39 (1974) 269–283.

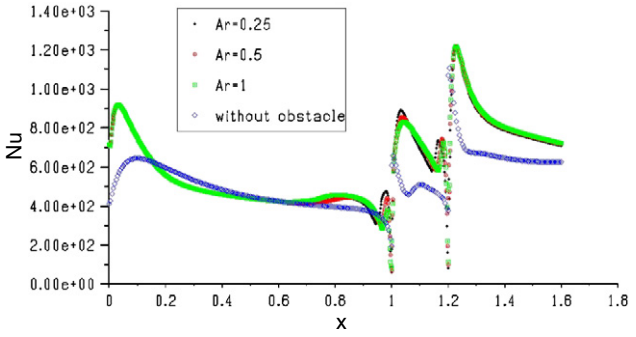

Fig. 9. Variation of local Nusselt number for different values of obstacle aspect ratio and for case 1 and Re = 30,000.

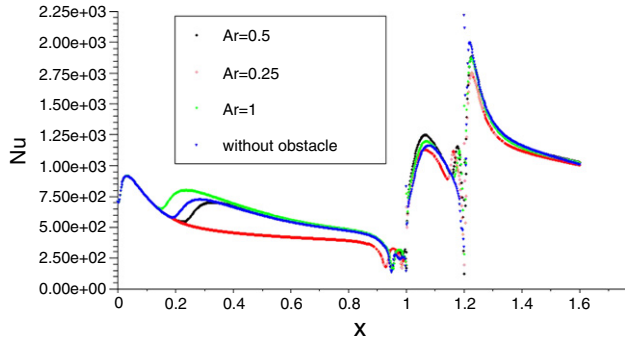

Fig. 10. Variation of local Nusselt number for different values of obstacle aspect ratio and for case 2 and Re = 30,000.

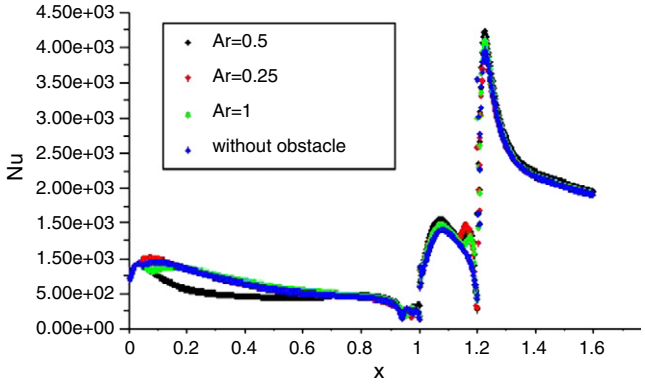

Fig. 11. Variation of local Nusselt number for different values of obstacle aspect ratio and for case 3 and Re = 30,000.

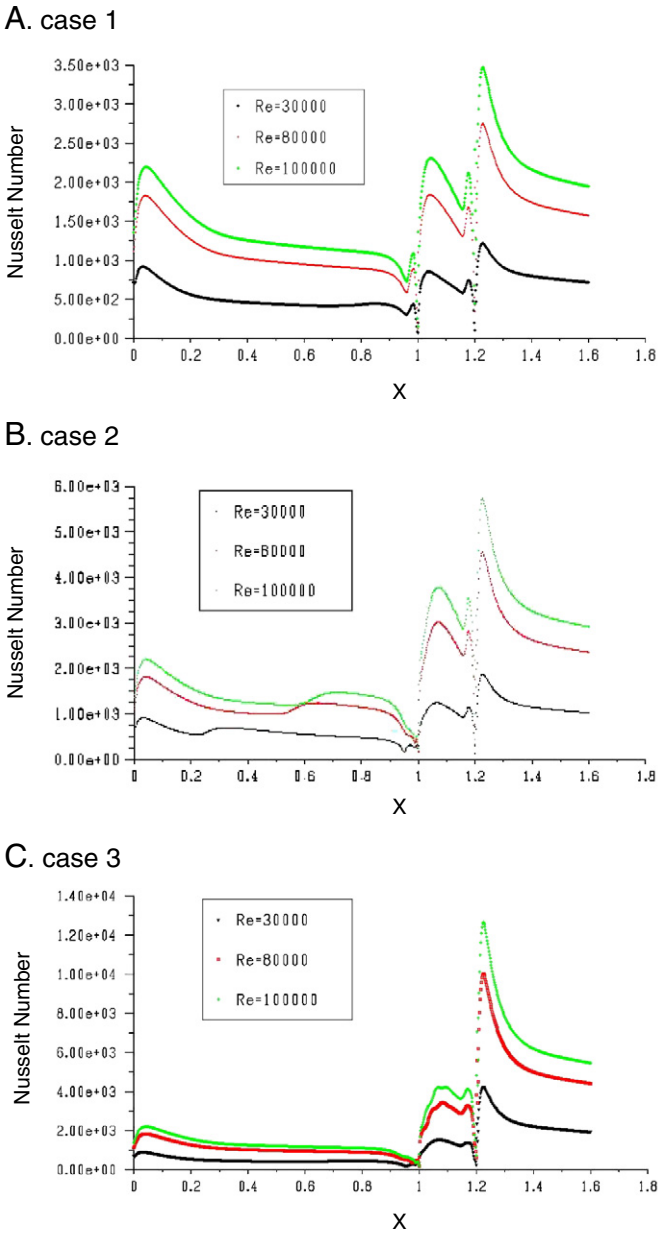

Fig. 12. Nusselt number variation for different values of Reynolds number and Ar = 0.5.

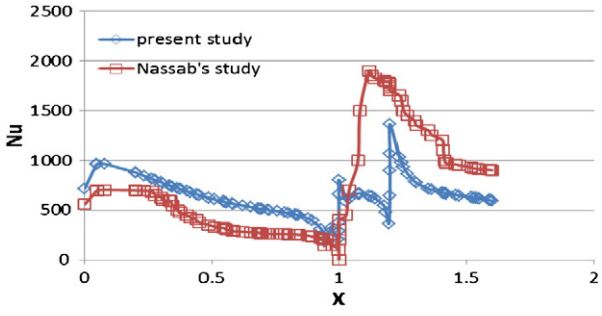

Fig. 13. Comparison with published results of Nassab et al. [3] for Re = 30,000, S/H = 0.7 and $\theta = 80°$.

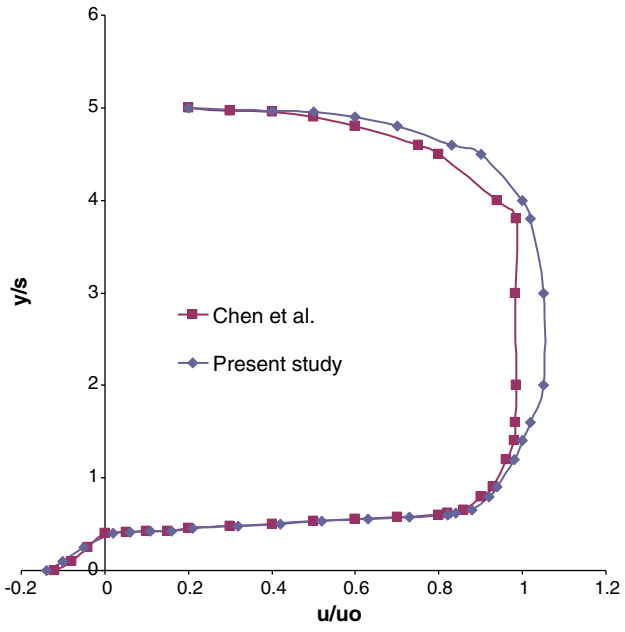

Fig. 14. Comparison with published results of Chen et al. [16] for ER = 1.11.